JOURNAL OF MATERIALS SCIENCE 32 (1997) 5669–5677

Studies of crystallization kinetics of $Fe_{40}Ni_{40}P_{14}B_6$ and $Fe_{80}B_{20}$ metallic glasses under non-isothermal conditions

V. I. TKATCH, A. I. LIMANOVSKII, V. YU. KAMENEVA
Physics and Engineering Institute, National Ukrainian Academy of Sciences, 340114 Donetsk, Ukraine

A model for the glass crystallization at constant rate heating is presented. Based on the model a technique for determination of the constants involved in the classical equations for the rates of homogeneous nucleation and linear crystal growth is derived. The effect of the heating rate (in the wide range from 2×10^{-2} to 16 $K s^{-1}$) on the temperature of crystallization as well as on the average grain size in fully crystallized specimens of $Fe_{40}Ni_{40}P_{14}B_6$ and $Fe_{80}B_{20}$ metallic glasses has been studied. The values of the interface diffusion coefficient, the rates of nucleation and growth and the volume density of quenched-in nuclei deduced in the present study are in good agreement with those derived from direct observations. It has been confirmed that crystallization of $Fe_{80}B_{20}$ occurs mainly by the three-dimensional growth of the pre-existing crystallites while the Avrami exponent for the $Fe_{40}Ni_{40}P_{14}B_6$ glass exceeds 4 implying non-steady-state nucleation. It has been demonstrated that the proposed model allows one to generalize the isothermal and non-isothermal kinetic crystallization curves.

1. Introduction

Crystallization studies of metallic glasses are of interest in understanding mechanisms of phase transformations far from equilibrium, evaluating the glass-forming ability of the melts, predicting the stability of the amorphous states as well as in producing controlled (mainly ultrarefined) microstructures. This process has been extensively studied for many years. Despite the numerous papers on crystallization and several comprehensive reviews (see, for example, [1, 2]) there is still no clear understanding of some aspects of this process [3].

The description of metallic glass crystallization requires both the appropriate kinetic equation and the values of the parameters included. These problems are interrelated since the most usual way to determine the kinetic parameters is to compare the experimental data and the predictions of theoretical models. However, until now the technique of evaluation of the kinetic parameters especially in the case of non-isothermal experiments (which are more accurate than isothermal experiments) is not universally accepted. This problem has been discussed earlier [4, 5] and it has been shown that a generalization is possible when the rate equation is invariant under any thermal conditions. In any case the existing methods of evaluation of kinetic parameters allow one to estimate the overall activation energy of crystallization, while it is important to determine the rates of crystal nucleation and growth. Earlier it has been shown [6, 7] that using the experimental dependences for both the crystallization temperature and the average grain size in crystallized specimens versus the heating rate it is possible to evaluate all necessary quantities involved in the classical equations for the rates of homogeneous nucleation and growth of crystals.

It should be noted that crystallization process in metallic glasses is complicated owing to both the presence of "quenched-in" crystallites which formed during rapid quenching and the transient behaviour of nucleation [8, 9]. For these reasons there is a large scatter of the experimental data (e.g., see the review in [8]).

The aims of the present paper are to generalize the method of treatment of the non-isothermal crystallization data, taking into account not only the population of the pre-existing crystallites, but also the transient behaviour of nucleation, and also to compare the crystallization kinetics under isothermal and continuous heating conditions. The studies have been carried out with the well-known $Fe_{40}Ni_{40}P_{14}B_6$ and $Fe_{80}B_{20}$ metallic glasses. These glasses and their crystallization behaviour have been intensively studied by numerous workers (see, for example [1, 2, 6–8, 10–20]) and there is a large amount of experimental data for them.

2. Kinetic equations

The crystallization kinetics are usually described by the model equation, proposed by Kolmogorov [21],

Johnson and Mehl [22] and Avrami [23–25]:

$$X(t) = 1 - \exp[-\varphi(t)] \tag{1}$$

where X is the crystalline fraction transformed and $\varphi(t)$ is the extended volume, i.e., volume fraction transformed if there were no impingement [26]. In general, when crystallization occurs by the nucleation and growth of spherical crystals, for both isothermal and non-isothermal conditions $\varphi(t)$ may be written as [21]

$$\varphi(t) = \frac{4\pi}{3}\int_0^t I(t')\left(\int_{t'}^t U(t'')\,dt''\right)^3 dt' \tag{2}$$

where I is the nucleation rate, and U is the crystal growth rate.

For isothermal conditions the volume fraction transformed at time t is described by the Johnson–Mehl–Avrami equation [22–26]

$$X(t) = 1 - \exp[-(Kt)^n] = 1 - \exp\left[-\left(\frac{t}{\tau_c}\right)^n\right] \tag{3}$$

where n is the dimensionless Avrami exponent which depends on the crystallization mechanism, K is the reaction rate constant and $\tau_c\,(=K^{-1})$ is the characteristic crystallization time.

If isothermal crystallization occurs by nucleation and three-dimensional growth of crystallites and the rates of crystal nucleation and growth are time independent, Equation (3) may be written

$$X(t) = 1 - \exp\left(-\frac{\pi}{3} I U^3 t^4\right) \tag{4}$$

As was mentioned above, the metallic glasses prepared by rapid melt quenching contain quenched-in crystallites which influence the crystallization kinetics. Since the extended volumes are additive, the contribution of the pre-existing crystallites is taken into account in the overall crystallization kinetics by the additional term in Equation 4 [10], i.e.,

$$X(t) = 1 - \exp\left[-\frac{\pi}{3} U^3 t^3 (It + 4N_-)\right] \tag{5}$$

where N_- is the number of quenched-in nuclei per unit volume.

When crystallization of the glass occurs under continuous heating from a certain temperature T_0 at the rate $\alpha(T)$, the extended volume fraction transformed at temperature T (in the absence of the pre-existing crystallites) may be written as a function of temperature T as

$$\varphi(T) = \frac{4\pi}{3}\int_{T_0}^T \frac{I(T')}{\alpha(T)}\left(\int_{T'}^T \frac{U(T'')}{\alpha(T)}\,dT''\right)^3 dT' \tag{6}$$

In subsequent analysis we substitute into Equation 6 the classical expressions for the rates of crystal nucleation and growth [26, 27]:

$$I(T) = \left(\frac{N_0 D}{a_0^2}\right)\exp\left(-\frac{W^*}{kT}\right) = \frac{N_0}{\tau_0}\exp\left(-\frac{Q}{T}\right) f(T) \tag{7}$$

$$U(T) = \left(\frac{D}{a_0}\right)\left[1 - \exp\left(-\frac{\Delta G}{kT}\right)\right] = \frac{a_0}{\tau_0}\exp\left(-\frac{Q}{T}\right) F(T) \tag{8}$$

Here N_0 is the number of atoms per unit volume, a_0 is the average atomic diameter or length of diffusion jump, D is the diffusivity at the amorphous (liquid)–crystal interface, W^* is the free energy of the critical nucleus formation, Q is the activation energy for the diffusion, τ_0 is the pre-exponential factor of the characteristic diffusion time ($\tau = a_0/D$), ΔG is the Gibbs free-energy difference between the amorphous (liquid) and crystalline phases and k is the Boltzmann constant.

For the integration of Equation 6 we assume that in a rather narrow temperature interval of crystallization the functions designated as $f(T)$ and $F(T)$ in Equations 7 and 8, respectively, have relatively small changes in comparison with $\tau(T)$ and take their values at temperatures where the rate of crystallization has a maximum (T_p). This allows us [7] for α = constant to obtain an approximation of Equation 6 in the form

$$\varphi(T) = \frac{\pi}{3}\left(\frac{T^2}{\alpha Q \tau_c}\right)^4 \tag{9}$$

where

$$\tau_c = \frac{\tau_0}{[2f(T_p)F^3(T_p)]^{1/4}}\exp\left(\frac{Q}{T}\right) = \left(\frac{\pi}{3} I U^3\right)^{-1/4} \tag{10}$$

is the characteristic time crystallization.

Then, comparing Equation 9 with the expression for the extended volume in the case of isothermal crystallization in Equation 3, we can see that they formally coincide if we introduce the quantity

$$t_{\text{eff}} = \frac{T^2}{\alpha Q} \tag{11}$$

as a certain effective time for the case of continuous heating.

Substituting Equation 9 into Equation 1 and taking into account the pre-existing crystallites with the population N_-, we can write the approximate equation for kinetics of metallic glass crystallization under heating with constant rate α in the form [7]

$$X(T) = 1 - \exp\left\{-\frac{\pi}{3} U^3\left(\frac{T^2}{\alpha Q}\right)^3\left[I\left(\frac{T^2}{\alpha Q}\right) + 4N_-\right]\right\} \tag{12}$$

which is similar to the form of Equation 5 for an isothermal case.

The volume density N_+, of "new" crystallites, formed in the glass during continuous heating at the rate α from temperature T_0 to T is

$$N_+ = \alpha^{-1}\int_{T_0}^T I(T')[(1 - X(T')]\,dT' \tag{13}$$

Substitution of Equations 7, 8 and 12 into Equation 13 yields a cumbersome expression which is rather

difficult for analytical approximation. However, this problem is simplified for the following two limiting cases [7].

(i) The crystallization of the metallic glass occurs by the nucleation and growth of "new" crystals.

(ii) The crystallization is controlled by the growth of pre-existing crystallites.

In other words it means that one of two terms in the exponent of Equation 12 is neglected. In the first case, when $I(t)(T^2/\mathrm{d}Q) \gg 4N_-$, Equation 13 may be approximated as

$$N_{+1} \approx 0.35 N_0 \left(\frac{2f(T_p)}{F(T_p)}\right)^{3/4} \quad (14)$$

If this is the case, when crystallization of the glass occurs mainly by the growth of quenched-in nuclei, the population of the "new" crystallites versus crystallization temperature can be expressed as

$$N_{+2} \approx 0.2 N_0^{4/3} \left(\frac{2f(T_p)}{F(T_p)}\right) N_-^{-1/3} \quad (15)$$

As can be seen from Equations 14 and 15 in any case the total population of crystallites in crystallized glasses ($N = N_- + N_+$) is a function of the crystallization temperature, T_p, which, in turn, depends on the heating rate α.

Therefore microstructural investigations of the crystallized glasses are very important in determination of the parameters of kinetic equations.

3. Experimental procedure and results

Glassy ribbons with nominal compositions $Fe_{40}Ni_{40}P_{14}B_6$ and $Fe_{80}B_{20}$ were prepared by melt spinning from a quartz nozzle into a roller made of aluminium bronze (diameter, 220 mm; surface speed, 25 m s^{-1}) in air. The quartz nozzle with a circular orifice of diameter 1 mm was positioned about 0.15 mm above the casting surface. The ejection pressure and melt superheat were 20 kPa and 100 K, respectively. The ribbons were 25 μm thick, about 1.5 mm wide and 5–7 m long.

X-ray diffraction (Fe$K\alpha$ radiation) was used to check amorphicity of the as-quenched ribbons as well as to identify the phase composition of crystallized specimens. The microstructure of the crystallized ribbons after etching by 5% Nital was studied by optical metallography.

The rate of heating was varied in the wide range from 2×10^{-2} to 16 K s^{-1}. The temperature was measured with a chromel–alumel thermocouple (diameter, about 50 μm) mounted in contact with the specimen. The accuracy in T was ± 1 K, the error in the measurements of resistance changes did not exceed 0.1% and the constancy of the heating rates was maintained within 5% by special control device.

The crystallization kinetics as shown by $X(T)$ were determined from electrical resistance, R, measurements assuming that relative changes in R vary linearly with volume fraction transformed. The electrical resistance was measured using a standard four-probe direct-current (d.c.) method. The equivalency (within

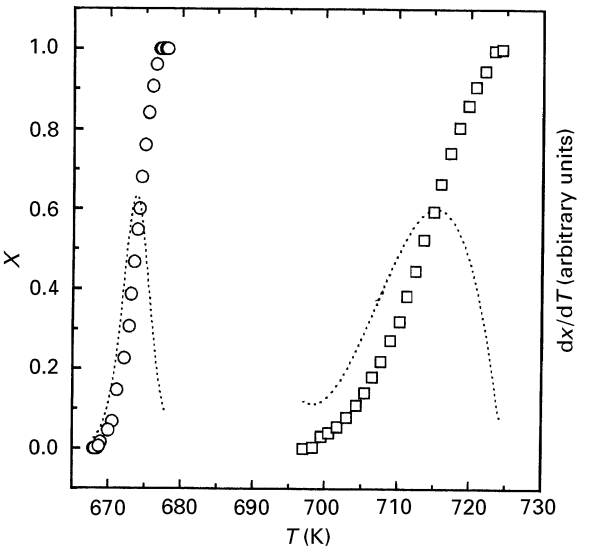

Figure 1 The transformed fraction, X, of amorphous $Fe_{40}Ni_{40}P_{14}B_6$ (○) and $Fe_{80}B_{20}$ (□) alloys calculated from the normalized resistance changes as a function of temperature at a heating rate of 0.17 K s^{-1}. The rates of transformation, $\mathrm{d}X/\mathrm{d}T$, are in arbitrary units calculated from the experimental data and presented by the dotted curves have maxima at $X \approx 0.63$.

the experimental error) of the functions $X(T)$ and $(R_0 - R)/(R_0 - R_\infty)$ was confirmed by the differential thermal analysis of several specimens. Here R_0 and R_∞ are the values of specimen resistance in the amorphous and completely crystallized states, respectively.

Additionally, using the cell of the differential thermal analysis apparatus, several measurements of the resistance changes at constant temperature were performed.

Fig. 1 illustrates two crystallization kinetic curves $X(T)$ for $Fe_{40}Ni_{40}P_{14}B_6$ and $Fe_{80}B_{20}$ glasses calculated from the changes in resistance at a heating rate 0.17 K s^{-1}. It can be seen that the $X(T)$ curves have a sigmoidal form typical of one-stage transformation. In contrast with the work of Greer [8] we have not observed a delay of crystallization for $Fe_{80}B_{20}$ glass. The relative homogeneity of the as-quenched structure of $Fe_{80}B_{20}$ specimens used in the present study may be due to the relatively low heat conductivity of the quenching roller made of aluminium bronze.

As has been shown [5, 7] for linear-heating crystallization the maximum rate of transformation always takes place at $X(T) = 0.63$. So we have calculated the crystallization rate, $\mathrm{d}X/\mathrm{d}T$, by numerical differentiation of the experimental kinetic curves with respect to T. The resulting curves shown by dotted curves in Fig. 1 have their maxima, T_p, at $X(T) \approx 0.63$. Note that the so-obtained temperatures of maximum crystallization rate for $Fe_{40}Ni_{40}P_{14}B_6$ (674.3 K) and for $Fe_{80}B_{20}$ (715 K) glasses are in a reasonable agreement with corresponding differential scanning calorimetry (DSC) data of Wang *et al.* [11] (677 K), Russev *et al.* [12] (676.3 K) for $Fe_{40}Ni_{40}P_{14}B_6$ glass and of Greer [8] (710 and 718 K for $Fe_{80}B_{20}$ ribbons of different thicknesses) obtained at a heating rate of 0.167 K s^{-1}. Such a correspondence may be considered as justification for the procedure used to determine the

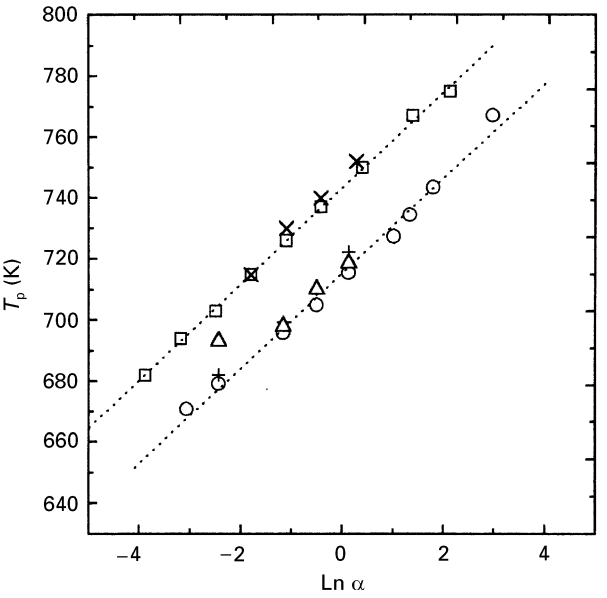

Figure 2 Crystallization temperatures, T_p, versus logarithm of heating rate, α, of $Fe_{40}Ni_{40}P_{14}B_6$ (○) and $Fe_{80}B_{20}$ (□) glasses estimated from the resistance changes data. The dotted lines are the results of the linear interpolation. The corresponding DSC data are taken from [11] (+), from [12] (△) and from [8] (×).

temperature, T_p, of the maximum rate of crystallization, as the temperature at which the normalized resistance is 0.63.

The so-determined values of T_p for $Fe_{40}Ni_{40}P_{14}B_6$ and $Fe_{80}B_{20}$ metallic glasses as functions of the heating rate are shown in Fig. 2. The measurements have shown that the value of T_p for $Fe_{40}Ni_{40}P_{14}B_6$ amorphous alloy increased from 653.6 to 733 K with α in the range from 2×10^{-2} to 16 K s^{-1} and that for $Fe_{80}B_{20}$ from 682 to 775 K for α ranging from 2×10^{-2} to 8.5 K s^{-1}. The increase in T_p is monotonic and may be approximated by straight lines against ln α. Again, as can be seen in Fig. 2, these data are in rather close agreement with DSC estimations of T_p in the narrower range of heating rates, reported by Wang *et al.* [11] and Russev *et al.* [12] (except for one point) for $Fe_{40}Ni_{40}P_{14}B_6$ glass as well as by Greer [8] for $Fe_{80}B_{20}$ amorphous alloy.

The X-ray diffraction studies of the specimens crystallized in the overall range of the heating rates show the presence of two phases: Fe–Ni austenite and $(FeNi)_3(PB)$ phase in $Fe_{40}Ni_{40}P_{14}B_6$ alloy and α-iron and tetragonal Fe_3B phase in $Fe_{80}B_{20}$ alloy. These observations also agree with the well-established data for these alloys (see, for example, [2, 8, 13]).

It has also been observed that the heating rate influences the average grain sizes, $\bar{L}$, estimated from optical micrographs of the crystallized specimens. That is, the increase in heating rate from 2×10^{-2} to 4.4 K s^{-1} (T_p increases from 654 to 714 K) leads to the increase in $\bar{L}$ in $Fe_{40}Ni_{40}P_{14}B_6$ alloy from 0.9 ± 0.05 to 1.4 ± 0.07 μm, which corresponds to changes in the average volume density of crystallites, N ($=\bar{L}^{-1/3}$), from 1.4×10^{18} to 3.6×10^{17} m^{-3}. In contrast, the average grain size in crystallized $Fe_{80}B_{20}$ specimens versus the heating rate changes in opposite direction; it decreases from 0.9 ± 0.05 μm (1.4×10^{18} m^{-3}) to 0.55 ± 0.05 μm (6×10^{18} m^{-3}) as α increases from 2×10^{-2} to 1.5 K s^{-1} and T_p ranges from 682 to 751 K. Note that the results of these rather rough estimates of $\bar{L}$ agree with the corresponding data obtained by transmission electron microscopy (TEM) for $Fe_{40}Ni_{40}P_{14}B_6$ [13] and $Fe_{80}B_{20}$ [8] metallic glasses.

The agreement between the experimental data described in this section and the data in the above cited papers implies that compositions of $Fe_{40}Ni_{40}P_{14}B_6$ and $Fe_{80}B_{20}$ glasses prepared in this study are close to the nominal and provides the basis for a subsequent comparison of different characteristics derived in the next section with the data obtained from direct observations.

4. Discussion

The apparently one-stage character of the transformation curves of $Fe_{40}Ni_{40}P_{14}B_6$ and $Fe_{80}B_{20}$ glasses (Fig. 1) and two-phase structure of crystallized specimens imply that crystallization of these glasses occurs by eutectic mechanism as was described in detail by Morris [13] and Greer [8], respectively. In this case there is no overall composition change between glass and an individual eutectic colony; so it is reasonable to assume that crystallization kinetics may be formally described using equations from Section 2. We are aware that such simplification ignores some features of the eutectic crystallization, and the physical meaning of the quantities involved in these and subsequent equations must be considered as effective.

Note that the monotonic behaviour of the values of T_p and N as functions of heating rate suggests that the mechanisms of crystallization in $Fe_{40}Ni_{40}P_{14}B_6$ and $Fe_{80}B_{20}$ remain unchanged over the range of α studied.

The choice of the maximum crystallization rate temperature, T_p ($X=0.63$), as a crystallization temperature means that the exponent in Equation 12 equals 1. Using the values of T_p the overall activation energy of crystallization under continuous heating at constant rate α may be estimated by several methods [4, 5, 28], but the most frequently used is that proposed by Kissinger [29]. If we, by analogy with Kissinger, replot the data presented in Fig. 2 as $\ln(T_p^2/\alpha)$ versus $(1/T_p)$, the slopes of the straight lines in Fig. 3 give us the values of the activation energies for crystallization of $Fe_{40}Ni_{40}P_{14}B_6$ and $Fe_{80}B_{20}$ glasses: $39\,600\pm1050$ K and $31\,300\pm700$ K, respectively. These values are in a reasonable agreement with values quoted for both $Fe_{40}Ni_{40}P_{14}B_6$, namely 37 000 K [11], and 44 160 K [14], and $Fe_{80}B_{20}$, namely 29 000 K [8].

On the other hand, as was shown earlier [7], substitution of Equations 7 and 8 into Equation 12 for two limiting cases, i.e., $I(T)(T^2/\alpha Q)\gg 4N_-$ and $I(T)(T^2/\alpha Q)\ll 4N_-$ gives, respectively,

$$\ln\left(\frac{T_p^2}{\alpha}\right)+\frac{1}{4}\ln\left[2f(T_p)F^3(T_p)\right]=\ln(Q_1\tau_{01})+\frac{Q_1}{T_p} \quad (16)$$

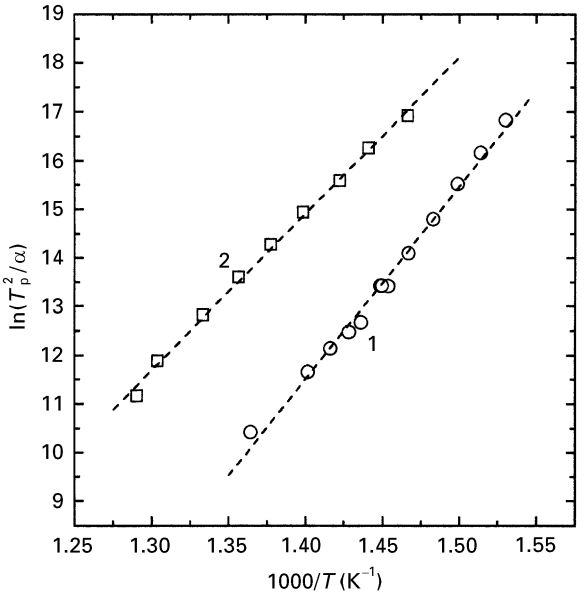

Figure 3 Kissinger plots derived from crystallization peak temperatures, T_p, for $Fe_{40}Ni_{40}P_{14}B_6$ (○) and $Fe_{80}B_{20}$ (□) glasses from data in Fig. 2. The gradients of the dashed lines are as follows; line 1, 39 600 ± 1050 K; line 2, 31 700 ± 700 K.

$$\ln\left(\frac{T_p^2}{\alpha}\right) = \ln\left[2f(T_p)\left(\frac{N_-}{N_0}\right)^{1/3}\right] = \ln(Q_2\tau_{02}) + \frac{Q_2}{T_p} \tag{17}$$

As it follows from Equations 16 and 17, their left-hand sides must be linear functions of $1/T_p$. Equations 16 and 17 are more complicated in comparison with the Kissinger relation, but they allow us to estimate also the activation energy Q, of diffusion, and the value of the pre-exponential factor, τ_{0i}. However, prior to applying this analysis to the experimental data for $T_p(\alpha)$ we have to estimate the values of functions denoted as $f(T)$ and $F(T)$ in Equations 7 and 8, respectively. This estimation may be done using the values of the number, N, of grains per unit volume in fully crystallized specimens.

As can be seen from Equations 14 and 15 the population of the crystallites formed during continuous heating depends on both $f(T_p)$ and $F(T_p)$. Let us consider these functions in detail. In classical theory the free energy of critical nucleus formation may be written as [26, 27]

$$W^* = \frac{16\pi\sigma^3 V^2}{3(\Delta G)^2} \tag{18}$$

where σ is the crystal–liquid (amorphous) interfacial energy per unit area, V is the molar volume and ΔG is the molar Gibbs free energy difference between the liquid (amorphous) and crystal phases. In order to estimate the values of W^*, one needs to know the values of σ and ΔG as well as their temperature dependences. For analysis of metallic glass crystallization the dependence of $\Delta G(T)$ is usually approximated by one of several models [30, 31], because for these materials the temperature dependences of the specific heats required for correct evaluation of ΔG are unknown. As for the value of σ, the two extreme cases may be considered: firstly, σ = constant and secondly $\sigma \propto T/T_m$ [32]. On the other hand, as has been shown earlier [6, 7], a comparison between the experimentally obtained values of the volume densities N, of the grains, in the specimens crystallized at different heating rates (and, therefore, at various T_p) and those calculated using Equations 14 and 15 allows us to choose the appropriate dependences $\sigma(T)$ and $\Delta G(T)$.

From results published earlier we assume that crystallization of $Fe_{40}Ni_{40}P_{14}B_6$ glass occurs by nucleation and growth of crystals in an amorphous matrix [2, 13], while $Fe_{80}B_{20}$ amorphous alloy transforms mainly by the growth of the quenched-in nuclei [8]. In other words, for $Fe_{40}Ni_{40}P_{14}B_6$ and $Fe_{80}B_{20}$ glasses we use Equations 14 and 15, respectively. The analysis shows that the experimentally observed changes in the average grain size versus T_p in crystallized $Fe_{40}Ni_{40}P_{14}B_6$ and $Fe_{80}B_{20}$ glasses may be satisfactorily approximated by the corresponding equations if σ is assumed to be constant and $\Delta G(T)$ is described by the equation proposed by Thompson and Spaepen [22], i.e.,

$$\Delta G = \frac{2\Delta H_m T(T_m - T)}{T_m(T_m + T)} \tag{19}$$

where ΔH_m is the molar heat of fusion. In this case the function $f(T)$ can be expressed as [6, 7]

$$f(\mathrm{T}) = \exp\left(\frac{-\varepsilon T_m^3(T_m + T)^2}{T^3(T_m - T)^2}\right) \tag{20}$$

with

$$\varepsilon = \frac{4\pi V^2\sigma^3}{3k\mathrm{T}_m(\Delta H_m)^2} \tag{21}$$

which is temperature independent, V being the molar volume.

The function denoted as $F(T)$ in Equation 8 may be written as

$$F(T) = 1 - \exp\left(-\frac{1.98(T_m - T)}{T_m + T}\right) \tag{22}$$

Besides the choice of the relevant model for $\Delta G(T)$ the fitting of the experimentally estimated values of $N(T_p)$ in the crystallized specimens allows us to calculate the values of ε for both alloys and to estimate the density, N_-, of the quenched-in nuclei in as-prepared amorphous $Fe_{80}B_{20}$. The calculated values are listed in Table I. In turn, substituting the values of the heats of fusion for $Fe_{40}Ni_{40}P_{14}B_6$ and $Fe_{80}B_{20}$ alloys from [16] and [17], respectively, into Equation 21 we have calculated the values of the interfacial free energy, σ (Table I). The value of σ ($=0.147\ \mathrm{J\,m^{-2}}$) derived in the present analysis for $Fe_{40}Ni_{40}P_{14}B_6$ alloy is in a reasonable agreement with the estimates earlier reported by Morris [13] (0.14–0.22 $\mathrm{J\,m^{-2}}$) and by Limoge and Barbu [18] (0.13 $\mathrm{J\,m^{-2}}$) and also the value of N_- ($7.3\times10^{17}\ \mathrm{m^{-3}}$) is in accordance with estimates in the range from 4×10^{17} to $3.6\times10^{18}\ \mathrm{m^{-3}}$ reported in [8, 20].

Using these data we have calculated the values of $f(T_p)$ and $F(T_p)$ and have replotted the data of $T_p(\alpha)$

TABLE I Estimated values of the parameters in Equations 7 and 8 for the rates of homogeneous nucleation and crystal growth in $Fe_{40}Ni_{40}P_{14}B_6$ and $Fe_{80}B_{20}$ glasses

Alloy	ε	σ (J m^{-2})	τ_0 (s)	Q (K)	N_- (m^{-3})
$Fe_{40}Ni_{40}P_{14}B_6$	0.469	0.147	5.2×10^{-31}	43 800	5×10^{13}
$Fe_{80}B_{20}$	0.437	0.2	7.5×10^{-22}	31 900	$(2–7)\times10^{7}$

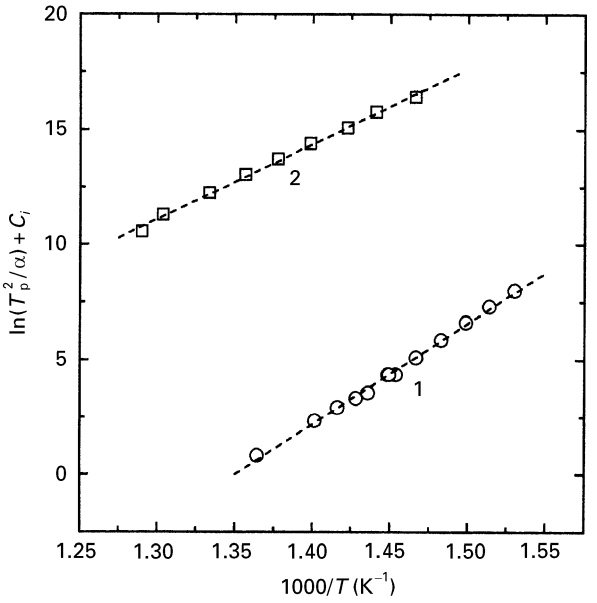

Figure 4 Modified Kissinger-type plots based on the following. (○), line 1, Equation 16 for $Fe_{40}Ni_{40}P_{14}B_6$ glass with $C_1 = \ln[2f(T_p)F^3(T_p)]^{1/4}$; (□), line 2, Equation 17 for $Fe_{80}B_{20}$ glass with $C_2 = \ln[2f(T_p)(N_-/N_0)^{1/3}]$. The slopes of the fitted broken lines are 43 800 ± 800 K for line 1 and 31 900 ± 700 K for line 2.

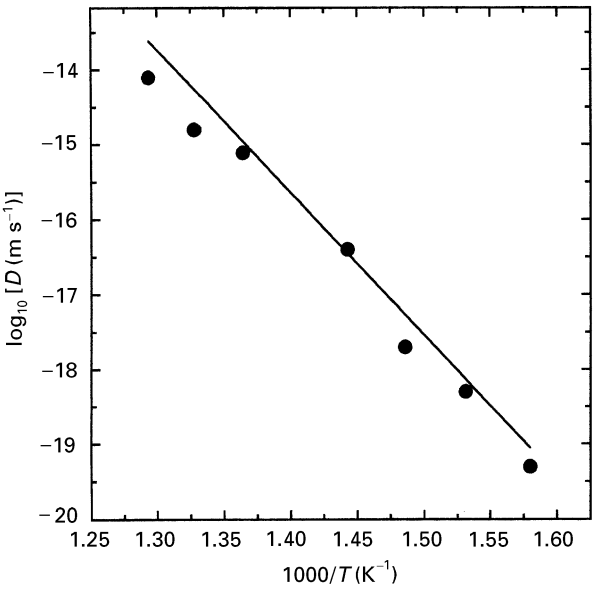

Figure 5 Comparison between diffusion coefficients in $Fe_{40}Ni_{40}P_{14}B_6$ glass deduced by Morris [19] from growth of boride (●) and those calculated in the present study on the basis of Arrhenius-type equation using the values of τ_0 and Q listed in Table I.

in Fig. 2 according to Equations 16 and 17 for $Fe_{40}Ni_{40}P_{14}B_6$ and $Fe_{80}B_{20}$ alloys, respectively. The results of this modified Kissinger-type analysis are presented in Fig. 4. As can be seen from Fig. 4 the calculated points are well approximated by linear dependences against $1/T$. The estimated slopes of these straight lines are 43 800 ± 800 K and 31 900 ± 700 K for $Fe_{40}Ni_{40}P_{14}B_6$ and $Fe_{80}B_{20}$ alloys, respectively. These values as well as the corresponding values of τ_0 estimated from intercept points are also listed in Table I. It should be noted that the value of the activation energy for the total crystallization process in $Fe_{80}B_{20}$ amorphous alloy estimated in Fig. 3 (31 300 K) is very close to that derived in the present analysis for the interfacial diffusion due to dominating role of crystal growth according to the assumed crystallization mode for this glass.

As follows from Equations 7 and 8 the so-derived parameters, Q and τ_0, describe the atomic diffusion across the glass–crystal interface assuming that D obeys an Arrhenius law. The dependence of $D(T)$ for $Fe_{40}Ni_{40}P_{14}B_6$ calculated using the data from Table I is in a good accordance with the values of diffusion coefficients estimated by Morris [19] from TEM studies of boride growth in the amorphous matrix (Fig. 5).

In order to provide a more comprehensive comparison of the results of presented analysis we have calculated the rates of crystal growth in both glasses by combining Equations 8 and 22 and using the values of Q and τ_0 from Table I. The calculated dependences of $U(T)$ shown by the solid and broken lines in Fig. 6 for $Fe_{40}Ni_{40}P_{14}B_6$ and $Fe_{80}B_{20}$ alloys, respectively, are in close agreement with the experimentally estimated values of eutectic growth rates reported by Morris [13, 19] and Limoge and Barbu [18] for $Fe_{40}Ni_{40}P_{14}B_6$ and by Greer [8] for $Fe_{80}B_{20}$.

Unfortunately, we have not found such reliable experimental data concerning the nucleation rates in these glasses. Nevertheless, the volume densities of quenched-in nuclei (about 5.0×10^{13} m^{-3} and 2×10^{17} m^{-3} for $Fe_{40}Ni_{40}P_{14}B_6$ and $Fe_{80}B_{20}$ glasses, respectively) estimated as

$$N_- = \alpha_q^{-1}\int_{T_0}^{T_m} I(T)\,dT \qquad (23)$$

using combination of Equations 6, 18 and 20 and the value of ε listed in Table I reasonably agree with the value of 10^{12} m^{-3} for $Fe_{40}Ni_{40}P_{14}B_6$ reported by Köster and Herold [20] and with the above cited values of N_- for $Fe_{80}B_{20}$. Here the mean quenching

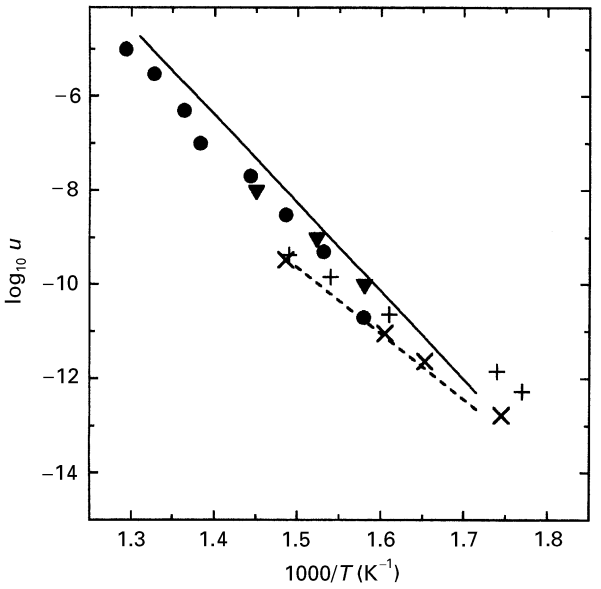

Figure 6 Calculated variations of crystal growth rates in $Fe_{40}Ni_{40}P_{14}B_6$ (——) and $Fe_{80}B_{20}$ (– – – –) glasses in comparison with the experimental data of Morris [13, 19] (●) and Limoge and Barbu [18] (▼) for $Fe_{40}Ni_{40}P_{14}B_6$ and Greer [8] (×) for $Fe_{80}B_{20}$.

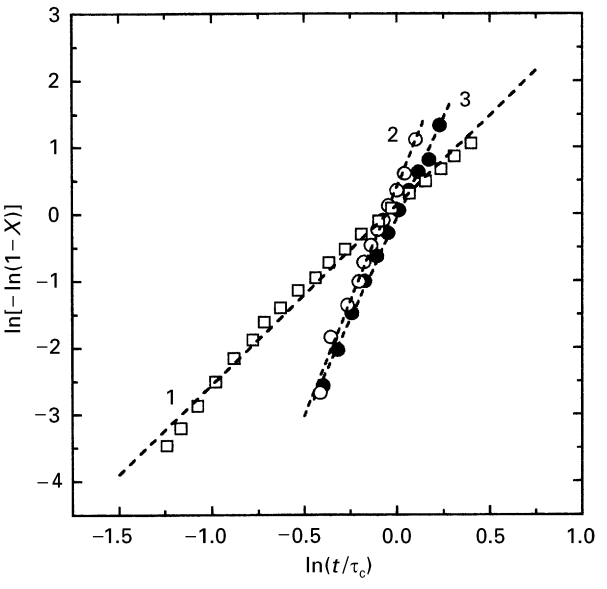

Figure 7 Plots of $\ln[-\ln(1-X)]$ versus $\ln(t/\tau_c)$ from isothermal (●) ($T = 640$ K) and non-isothermal (○, □) ($\alpha = 0.17$ K s^{-1}) experimental data for $Fe_{40}Ni_{40}P_{14}B_6$ (●, ○) and $Fe_{80}B_{20}$ (□) glasses. The least-squares linear approximations shown by the broken lines give the values of Avrami exponent, n: line 1, 2.7 ± 0.06; line 2, 6.9 ± 0.2, line 3, 6.0 ± 0.15. The original non-isothermal kinetic curves are shown in Fig. 1.

rate, α_q, was adopted to be 10^6 K s^{-1} and T_0 was taken to be $0.5T_m$. Note that both estimates of the quenched-in nuclei population in as-quenched $Fe_{80}B_{20}$ glass made in the present study give values of the same order. Besides this, a maximum of the calculated $I(T)$ dependence for $Fe_{40}Ni_{40}P_{14}B_6$ alloy (6×10^{17} m^{-3} s^{-1} at 763 K) is very close to that calculated by Morris [13] on the base of TEM observations.

Also it has been found that the functions denoted in Equation 7 as $f(T)$ and calculated according to Equations 21 and 22 for $Fe_{40}Ni_{40}P_{14}B_6$ and $Fe_{80}B_{20}$ alloys have maxima at approximately 628 K and 823 K, respectively. As has been shown in Section 3 the $Fe_{40}Ni_{40}P_{14}B_6$ glass crystallizes in the range 654–733 K, while the values of T_p for amorphous $Fe_{80}B_{20}$ alloy range from 682 to 775 K. This means that the free energy of formation of a critical nucleus in the former alloy increases while in the latter it decreases versus temperature in the ranges studied. These results of calculations are in accordance with experimentally observed behaviour of the average grain sizes in crystallized glasses versus heating rate described in Section 3. Thus, good agreement between the experimental data and the calculated values may be considered as a support for the procedure used here to estimate the values of the parameters which determine the rates of nucleation and crystal growth in metallic glasses.

In turn, knowledge of the $I(T)$ and $U(T)$ dependences, at least in the range of the glass crystallization temperatures, allows us to consider in detail the transformation mechanism and kinetics in $Fe_{40}Ni_{40}P_{14}B_6$ and $Fe_{80}B_{20}$ amorphous alloys at constant heating rate. Using the values of the effective time (Equation 11) for the case of continuous heating and the crystallization time (Equation 10) we may analyse the experimental kinetic curves $X(T)$ in terms of the equation

$$X(T) = 1 - \exp\left[-\left(\frac{t_{eff}}{\tau_c}\right)^n\right] \qquad (24)$$

which is similar to the Johnson–Mehl–Avrami expression for isothermal crystallization (Equation 3). Fig. 7 illustrates the results of replotting the kinetic curves for $Fe_{40}Ni_{40}P_{14}B_6$ (line 2) and $Fe_{80}B_{20}$ (line 1) glasses shown in Fig. 1 as $\ln\{-\ln[1 - X(T)]\}$ vs $\ln(t_{eff}/\tau_c)$. The so-obtained dependences (open symbols in Fig. 7) are close to linear dependences with the slopes $n = 6.9 \pm 0.2$ for $Fe_{40}Ni_{40}P_{14}B_6$ and $n = 2.7 \pm 0.06$ for $Fe_{80}B_{20}$ metallic glass. The last value of n is very close to the value of 2.8 obtained by Greer [8] from isothermal DSC studies of $Fe_{80}B_{20}$ crystallization and, in turn, close to the value of 3, which implies glass crystallization by the three-dimensional growth of pre-existing crystallites at zero nucleation rate. Note that this mode of crystallization was assumed above for this alloy in evaluating the values of Q, τ_0 and N_- by Equation 17.

The high value of exponent n (>4) obtained for the non-isothermal kinetic crystallization curve of $Fe_{40}Ni_{40}P_{14}B_6$ glass in Fig. 7 may result from either an increasing rate of nucleation (non-steady-state process) or incorrect analysis described above. To consider this problem in detail we have plotted the isothermal kinetic curve obtained for $Fe_{40}Ni_{40}P_{14}B_6$ glass at 640 K as $\ln\{-\ln[1 - X(t)]\}$ against $\ln(t/\tau_c)$ in accordance with Equation 3. As can be seen from Fig. 7, the Johnson–Mehl–Avrami plot (full circles and line 3) is linear with the slope $n = 6.0 \pm 0.15$. Note that in this case the possible errors involved in calculations of τ_c do not influence the slope of the resulting line which is essentially higher than the earlier reported values of 3.0 [12] and 3.5–4.0 [15].

The other reason for the relatively high values of exponent n revealed in $Fe_{40}Ni_{40}P_{14}B_6$ glass may be due to transient nucleation [9, 26] which arises because it takes some time to establish an equilibrium distribution of embryos. Several theoretical approaches of non-steady-state nucleation have been considered by James [33]. On the basis of his results we use in subsequent analysis the treatment proposed by Kashchiev [34]. According to Kashchiev the rate, I_{ns}, of non-steady-state nucleation is given by

$$I_{ns} = I\left[1 + 2\sum_{m=1}^{\infty}(-1)^m \exp\left(-\frac{m^2 t}{\tau_{ns}}\right)\right] \quad (25)$$

where m is an integer and τ_{ns} is the induction time.

In further analysis we have attempted to describe the experimental kinetic crystallization curves for $Fe_{40}Ni_{40}P_{14}B_6$ glass for isothermal and non-isothermal conditions by Equations 5 and 12, respectively, using I_{ns} as given by Equation 25 with τ_{ns} as an adjustable parameter. In this analysis according to Thompson *et al.* [9] and James [33] we have assumed that the temperature dependence of τ_{ns} follows an Arrhenius behaviour with the activation energy equal to that for interfacial diffusion, i.e., Q. The simulation has shown that introducing the induction time into the kinetic equations shifts the calculated curves to larger values of time with respect to experimental data. We have compensated this shift by a slight decrease in the constant ε in Equation 20 (from 0.469 to 0.44), i.e., decrease in σ from 0.147 to 0.138 $J\,m^{-2}$. Additionally we have calculated the non-isothermal crystallization kinetic curve for $Fe_{80}B_{20}$ glass at $\alpha = 0.17\ K\,s^{-1}$ using Equation 12 and the parameters listed in Table I.

A comparison of the experimental and calculated kinetic curves is illustrated in Fig. 8. Here, similar to Fig. 7, the non-isothermal data are plotted against $\ln(t_{eff}/\tau_c)$ while to plot the isothermal curve we have used the values of real time t. It is noteworthy that both kinetic curves calculated for isothermal ($T = 640$ K; $\tau_{ns} = 3400$ s) and non-isothermal ($\alpha = 0.17\ K\,s^{-1}$) crystallization of $Fe_{40}Ni_{40}P_{14}B_6$ glass coincide within calculation errors. The slope of this joint curve accounting for transient nucleation is 4 (line 2 in Fig. 8).

The reasonable agreement between the experimental (symbols) and calculated (solid lines) kinetic curves in Fig. 8 indicates that both Equation 12 and the constants derived in the present study are available for the description of crystallization kinetics in $Fe_{40}Ni_{40}P_{14}B_6$ and $Fe_{80}B_{20}$ glasses on continuous heating. It is evident that the high values of the Avrami exponent ($n > 4$) derived in Fig. 7 for $Fe_{40}Ni_{40}P_{14}B_6$ glass are caused by the non-steady-state nucleation. Finally, the coincidence of the calculated isothermal and non-isothermal kinetic curves as well as the observed proximity of the experimental curves (taking into account uncertainties related with the heating time in the isothermal experiment) imply that using the quantity $T^2/\alpha Q$ as an effective time in the case of linear heating allows us to generalize the treatment of isothermal and non-isothermal crystallization of metallic glasses. It is also interesting to note that the Avrami exponent of the calculated $X(T)$ kinetic curve for $Fe_{80}B_{20}$ glass (line 1 in Fig. 8) is 2.9, i.e., somewhat lower than 3.

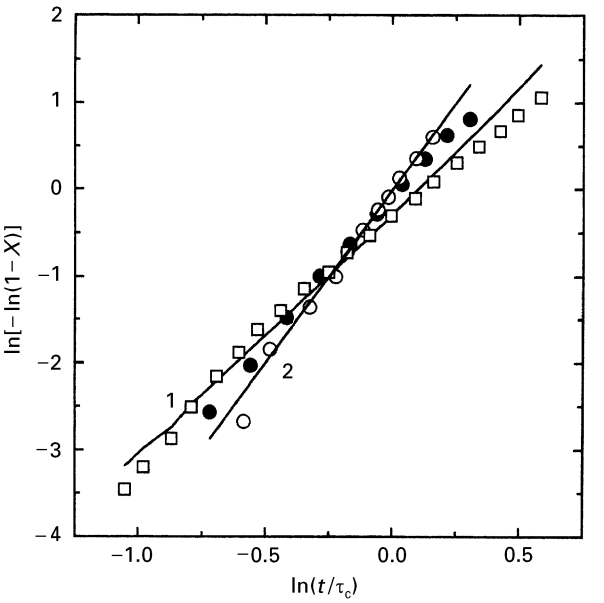

Figure 8 A comparison of the experimental kinetic curves shown in Fig. 7 (○, ●, □) and the curves calculated using Equations 5 and 12 for isothermal and non-isothermal crystallization, respectively (lines 1 and 2). The kinetic transformation curves of $Fe_{40}Ni_{40}P_{14}B_6$ glass calculated for annealing at 640 K as well as for continuous heating rate with $\alpha = 0.17\ K\,s^{-1}$ and accounting for the non-steady-state nucleation (Equation 25) coincide and have the slope 4. The slope of the kinetic line 1 calculated for $Fe_{80}B_{20}$ glass using Equation 12 is 2.9.

A more rigorous quantitative analysis of the transient effects in $Fe_{40}Ni_{40}P_{14}B_6$ amorphous alloy requires additional experimental studies which are now in progress.

5. Conclusions

1. It has been shown that by using the parameter $T^2/Q\alpha$ as an effective time a kinetic equation for glass crystallization controlled by nucleation and growth under continuous heating may be written in the form equivalent to the widely used Johnson–Mehl–Avrami equation for isothermal conditions. This means that in this case the isokinetic hypothesis is a reasonable approximation.

2. It was found that in the wide range of heating rates from 2×10^{-2} to16 $K\,s^{-1}$ the temperature, T_p, of the maximum rate of crystallization of $Fe_{40}Ni_{40}P_{14}B_6$ and $Fe_{80}B_{20}$ amorphous alloys monotonically increased (about 100 K), implying unchanged modes of crystallization. The average grain size, $\bar{L}$, in crystallized specimens of $Fe_{40}Ni_{40}P_{14}B_6$ glass increases with increasing heating rate while, in $Fe_{80}B_{20}$, $\bar{L}$ changes in the opposite direction. Based on these data and assuming the Thompson–Spaepen model for the temperature dependence of the amorphous–crystalline free-energy difference and constancy of the interfacial free energy, σ, the values of σ were estimated to be 0.147 $J\,m^{-2}$ and 0.2 $J\,m^{-2}$ for $Fe_{40}Ni_{40}P_{14}B_6$ and $Fe_{80}B_{20}$ glasses, respectively.

3. Using these data and the modified Kissinger-type equation presented in the study the activation energies and pre-exponential factors for the Arrhenius-type equation of interfacial diffusion have been estimated. The values of Q (43 800 and 31 900 K for $Fe_{40}Ni_{40}P_{14}B_6$ and $Fe_{80}B_{20}$, respectively) as well as the calculated rates of crystal (eutectic) growth and the numbers of quenched-in nuclei (5×10^{13} and $(2–7) \times 10^{17}$ in $Fe_{40}Ni_{40}P_{14}B_6$ and $Fe_{80}B_{20}$ as-quenched glasses, respectively) are in reasonable agreement with the results of direct observations published earlier.

4. The value of the Avrami exponent of the kinetic curve $X(T)$ for $Fe_{80}B_{20}$ glass is 2.7 which is in accordance with the well-established (for this amorphous alloy) crystallization mechanism occurring by growth on pre-existing nuclei. In contrast, the values of the Avrami exponent estimated from experimental isothermal and non-isothermal kinetic curves of $Fe_{40}Ni_{40}P_{14}B_6$ and 6.0 and 6.9, respectively, suggesting non-steady-state nucleation in this glass. This suggestion has been confirmed by matching the experimental kinetic curves and calculated data using the model equations. The value of the induction time for transient nucleation at 640 K estimated from the fitting is 3400 s.

5. The experimental isothermal and non-isothermal kinetic curves for $Fe_{40}Ni_{40}P_{14}B_6$ metallic glass are very close while the calculated data coincide, being plotted versus t/τ_c and t_{eff}/τ_c, respectively, and have the Avrami exponent 4, i.e., using the effective time allows a generalized description of crystallization kinetics under isothermal and linear heating conditions.

Acknowledgements

The research described in this publication was supported in part by Grant U1F200 from the Joint Fund of the Government of Ukraine and International Science Foundation.

References

1. U. KÖSTER and U. HEROLD, in "Metallic glasses", edited by H. -J. Güntherodt and H. Beck (Springer, Berlin, 1981) p. 225.
2. M. G. SCOTT, in "Amorphous metallic alloys" edited by Fluborsky (Butterworth, Amsterdam, 1983) p. 169.
3. A. L. GREER, *Mater. Sci. Engng* **A179–A180** (1994) 41.
4. H. YINNON and D. R. UHLMANN, *J. Non-Cryst. Solids* **54** (1983) 253.
5. T. KEMENY and J. SESTAK, *Thermochim. Acta* **110** (1987) 113.
6. V. P. NABEREZHNYKH, V. I. TKATCH, A. I. LIMANOVSKII, L. V. KUKSA and V. Yu. KAMENEVA, *Fiz. Metall. Metalloved.* **66** (1988) 169.
7. V. P. NABEREZHNYKH, V. I. TKATCH, A. I. LIMANOVSKII and V. Yu. KAMENEVA, *ibid.* **2** (1991) 157.
8. A. L. GREER, *Acta Metall.* **30** (1982) 171.
9. C. V. THOMPSON, A. L. GREER and F. SPAEPEN, *ibid.* **34** (1983) 1883.
10. A. L. GREER, in Proceedings of the Fifth International Conference on Rapidly Quenched Metals, edited by S. Steeb and H. Warlimont (Elsevier, Amsterdam, 1985) p. 215.
11. J. WANG, Sh. WEI, B. DING and Sh. LI, in Proceedings of the Fourth International Conference on Rapidly Quenched Metals (Japan Institute of Metals, Sendai, 1982) p. 731.
12. K. RUSSEV, S. BUDUROV and L. ANESTIEV, in Proceedings of the Fifth International Conference on Rapidly Quenched Metals, edited by S. Steeb and H. Wasliment (Elsevier, Amsterdam, 1985) p. 283.
13. D. G. MORRIS, *Acta Metall.* **29** (1981) 1213.
14. C. ANTONIONE, L. BATTEZZATI, A. LUCCI, G. RIONTINO and G. VENTURELLO, *Scripta Metall.* **12** (1978) 1011.
15. M. G. SCOTT, *J. Mater. Sci.* **13** (1978) 291.
16. P. M. ANDERSON and A. E. LORD, *J. Non-Cryst. Solids* **37** (1980) 219.
17. H.-W. BERGMANN, H. U. FRITSH and G. HUNGER, *J. Mater. Sci.* **16** (1981) 1933.
18. Y. LIMOGE and A. BARBU, in Proceedings of the Fourth International Conference on Rapidly Quenched Metals (Japan Institute of Metals, Sendai, 1982) p. 739.
19. D. G. MORRIS, *Scripta Metall.* **16** (1982) 585.
20. U. KÖSTER and U. HEROLD, in Proceedings of the Fifth International Conference in Rapidly Quenched Metals, edited by S. Steeb and H. Wasliment (Elsevier, Amsterdam, 1985) p. 717.
21. A. N. KOLMOGOROV, *Izv. Akad. Nauk USSR, Ser. Matem.* **1** (1937) 355.
22. W. A. JOHNSON and K. F. MEHL, *Trans. AIME* **135** (1939) 416.
23. M. AVRAMI, *J. Chem. Phys.* **7** (1939) 1103.
24. *Idem, ibid.*, **8** (1940) 212.
25. *Idem, ibid.*, **9** (1941) 177.
26. J. W. CHRISTIAN, "The theory of transformations in metals and alloys" (Pergamon, New York, 2nd Edn, 1975).
27. D. R. UHLMANN, *J. Non-Cryst. Solids* **7** (1972) 337.
28. M. A. ABDEL-RAHIM, A. Y. ABDEL-LATIF, A. EL-KORASHY and G. A. MOHAMED, *J. Mater. Sci.* **30** (1995) 5737.
29. H. G. KISSINGER, *J. Res. Natl Bur. Stand.* **57** (1956) 217.
30. C. V. THOMPSON and F. SPAEPEN, *Acta Metall.* **27** (1979) 1855.
31. H. J. FECHT, *Mater. Sci. Engng* **A133** (1991) 443.
32. F. SPAEPEN and R. B. MEYER, *Scripta Metall.* **10** (1976) 37.
33. P. F. JAMES, *Phys. Chem. Glasses* **115** (1974) 95.
34. P. KASHCHIEV, *Surf. Sci.* **14** (1969) 209.

Received 7 October 1996
and accepted 1 May 1997